Integrated Robust Control of the Global Toroidal Rotation and Total Plasma Energy in Tokamaks

Andres Pajares and Eugenio Schuster

***Abstract*— Integrated-control solutions will play a significant role in future tokamaks, in which a variety of coupled control problems will need to be solved simultaneously by means of a limited number of actuators. In this article, the problem of simultaneously regulating the global toroidal rotation, Ω_ϕ, and total plasma energy, W, is tackled. These two 0-D variables, Ω_ϕ and W, depend on the ion toroidal rotation and electron temperature profiles, respectively. Both Ω_ϕ and W also depend on the electron density and safety factor profiles. The actuation methods considered in this article are co-current and counter-current neutral beam injection. A nonlinear, robust controller that makes use of Lyapunov redesign techniques is synthesized based on 0-D, control-oriented models of the Ω_ϕ and W dynamics. In addition, an actuator management scheme is designed to handle variations in the control priorities and availability of the neutral beam injectors. The actuator manager solves an optimization problem in real time in order to find the most appropriate course of action when unexpected changes occur. The integrated control architecture is tested for a DIII-D scenario by means of the 1-D code Control-Oriented Transport Simulator (COTSIM), which predicts the time evolution of the electron temperature, electron density, ion toroidal rotation, and safety factor profiles.**

***Index Terms*— Integrated control, nonlinear robust control, tokamaks.**

I. Introduction

IN TOKAMAK plasmas, the thermal energy per volume unit, E, and the ion toroidal angular velocity, ω_ϕ, are profiles of substantial interest [1]. The first one, E, is closely related to the ion and electron density and temperature profiles and, therefore, to the pressure, plasma β, and fusion triple product. All these variables characterize the plasma performance and are key for tokamaks to become economically competitive means of producing energy. The second one, ω_ϕ, is related to the ions toroidal momentum and, therefore, to their density and temperature as well. In addition, the triggering of numerous magnetohydrodynamic (MHD) instabilities is related to E and ω_ϕ, such as neoclassical tearing modes (NTMs) or resistive wall modes (RWMs), which may substantially decrease the plasma performance and/or terminate the plasma discharge.

As a result, active control of E and ω_ϕ is a problem of relevance in current nuclear-fusion research. Although rotation control may be limited in large tokamaks, such as ITER, due to their higher volume and inertia, it may be a relevant problem for compact fusion reactors, which will play a significant role in the future nuclear-fusion research. In any case, this control problem offers significant challenges. First, modeling the E and ω_ϕ dynamics for control design is not an easy task. Although complex models providing a significant degree of accuracy might be available, using such models for control design may be impractical or just impossible. Instead, employing reduced, control-oriented models may make the controller synthesis possible. Moreover, the number of available actuators is limited, and the tokamak's actuation capability may not allow for controlling whole 1-D profiles (such as E or ω_ϕ). Alternatively, it can be more realistic to control 0-D variables related to 1-D variables. For example, the stored thermal energy, denoted as W, and the bulk toroidal rotation, denoted as Ω_ϕ, are 0-D variables related to E and ω_ϕ, respectively.

Previous work on simultaneous control of W and Ω_ϕ can be found in [2]. In such work, a linear, data-driven model was employed, and a controller was synthesized using linear techniques. Previous work on controlling ω_ϕ (at least at one point) simultaneously with W can be found in [3] and [4] for DIII-D and in [5] for NSTX-U. Linear robust techniques are utilized in [3] and [4], whereas real-time optimization is used in [3], [4] after approximate linearization of the plasma dynamics.

In this article, a nonlinear, 0-D coupled model of the $\Omega_\phi - W$ dynamics is employed to design a multi-input multi-output (MIMO) nonlinear controller. Model uncertainties are included to account for the unknown and/or unmodeled dynamics neglected in the 0-D modeling process. A nominal stabilizing controller is designed by using nonlinear design techniques and later robustified by using Lyapunov redesign techniques, ensuring stability and performance despite model uncertainties. Regulation of $\Omega_\phi - W$ is carried out by means of neutral beam injection (NBI). The fact that this actuator affects both W and Ω_ϕ (by means of the heating power and torque injected), together with the coupled $\Omega_\phi - W$ dynamics, suggest that MIMO controllers will have improved performance compared with other approaches. No other auxiliary sources are considered (e.g., radio frequency antennas,

Manuscript received July 16, 2019; revised November 20, 2019; accepted January 19, 2020. Date of publication April 29, 2020; date of current version June 10, 2020. This work was supported by the U.S. Department of Energy, Office of Science, Office of Fusion Energy Sciences, using the DIII-D National Fusion Facility, a DOE Office of Science User Facility, under Award DE-SC0010661 and Award DE-FC02-04ER54698. The review of this article was arranged by Senior Editor G. H. Neilson. *(Corresponding author: Andres Pajares.)*

The authors are with the Department of Mechanical Engineering and Mechanics, Lehigh University, Bethlehem, PA 18015 USA (e-mail: andres.pajares@lehigh.edu).

Color versions of one or more of the figures in this article are available online at http://ieeexplore.ieee.org.

Digital Object Identifier 10.1109/TPS.2020.2987264

0093-3813 © 2020 IEEE. Personal use is permitted, but republication/redistribution requires IEEE permission.
See https://www.ieee.org/publications/rights/index.html for more information.

Authorized licensed use limited to: LEHIGH UNIVERSITY. Downloaded on July 13,2020 at 21:30:41 UTC from IEEE Xplore. Restrictions apply.

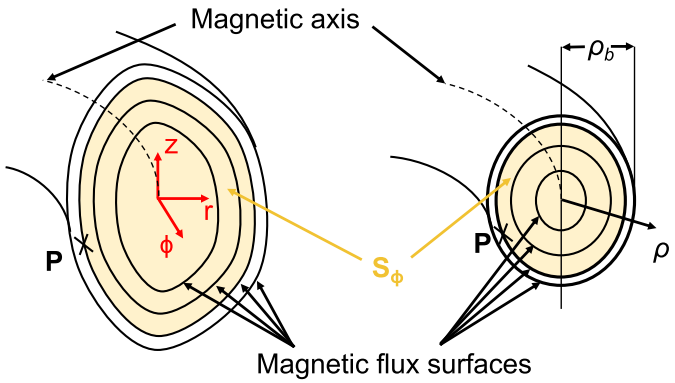

Fig. 1. Magnetic configuration in a tokamak under ideal MHD conditions.

such as electron-cyclotron (EC) heating) since assuming the availability of a larger number of actuators for this type of control problem, which would indeed make the control problem decoupled and rather trivial, is simply unrealistic in present and future tokamaks where these additional actuators need to be reserved for different control goals. In addition, future tokamaks will face changes in the plasma conditions, control objectives, and actuator availability that will require the implementation of supervisory systems with actuator management capabilities. For this reason, actuator management is added to the control scheme in order to handle possible variations in the control priorities and NBI availability (see our previous work [6]).

This article is organized as follows. The nonlinear model for the Ω_ϕ and W evolutions is described in Section II. The control design is presented in Section III. A simulation study to illustrate the performance of the 0-D controller in 1-D simulations for a DIII-D scenario is included in Section IV. Finally, a brief summary and possible future work are presented in Section V.

II. Global Toroidal Rotation and Total Plasma Energy Model

Under ideal MHD conditions, the magnetic-flux surfaces in a tokamak form toroidally nested surfaces around the magnetic axis (see Fig. 1). A magnetic-flux surface is defined by points with the same value of the toroidal flux, Φ, mean effective minor radius, ρ, poloidal magnetic flux, Ψ, pressure p, or others [1]. Only one of these functions (known as flux functions) is needed to index the magnetic-flux surfaces. This, together with the assumption of toroidal symmetry, reduces the 3-D problem in space (r–z–ϕ coordinates) to a 1-D problem. In this model, $\hat{\rho} = \rho/\rho_b$ is used as the flux function to label the magnetic-flux surfaces (where $\rho \triangleq (\Phi/(\pi B_{\phi,0}))^{1/2}$, $B_{\phi,0}$ is the toroidal magnetic field on axis, and ρ_b is the value of ρ at the last closed magnetic-flux surface, see Fig. 1).

The pressure field, p, is given by

$$p = n_e K T_e + n_i K T_i \tag{1}$$

where n_e and n_i are the electron and ion densities, respectively, T_e and T_i are the electron and ion temperatures, respectively, and K is Boltzmann's constant. It is assumed that the plasma is purely hydrogenic; therefore, the quasi-neutrality condition can be written as $n_e \approx n_i$, and (1) becomes $p = n_e K(T_e + T_i)$. The thermal energy density, E, is given by

$$E = \frac{3}{2} n_e K (T_e + T_i) = \frac{3}{2} p \tag{2}$$

so E is a constant in a magnetic-flux surface as well.

Although it has been shown that E is a flux function, it cannot be shown in general that the ion toroidal velocity, $v_{\phi,i}$, or ω_ϕ are flux functions as well. The ion toroidal angular velocity, ω_ϕ, is taken as $\omega_\phi = \langle v_{\phi,i} \rangle / R_0$, where R_0 is the tokamak's major radius (which is considered constant) and $\langle(\cdot)\rangle$ denotes the flux-surface average.

A. Thermal Stored Energy

The thermal stored energy, W, is the thermal energy contained within the last-closed magnetic-flux surface, and it is defined as

$$W(t) \triangleq \int_{V_p} E \, dV = \int_{\hat{\rho}=0}^{\hat{\rho}=1} E(\hat{\rho}, t) \frac{\partial V(\hat{\rho})}{\partial \hat{\rho}} d\hat{\rho} \tag{3}$$

where V_p is the plasma region enclosed within the last magnetic-flux surface and $V(\hat{\rho})$ is the plasma volume enclosed by the magnetic-flux surface at $\hat{\rho}$.

The model proposed in this article for the dynamics of W is based on a 0-D power balance in the plasma

$$\frac{dW}{dt} = -\frac{W}{\tau_E} + P_{\text{tot}} \tag{4}$$

where $P_{\text{tot}} = \sum_{i=1}^{i=N_{\text{NBI}}} P_{\text{NBI},i} + P_{EC}$ is the total injected power, $P_{\text{NBI},i}$ is the power corresponding to the i-th NBI, N_{NBI} is the total number of NBIs, P_{EC} is the total EC power, and τ_E is the energy-confinement time, which is modeled by the IPB98(y,2) scaling [7]

$$\tau_E = H_H \, k \, P_{\text{tot}}^{-0.69}, \tag{5}$$

$$k = 0.0562 I_p^{0.93} B_T^{0.15} R_0^{1.97} \kappa^{0.78} \epsilon^{0.58} M^{0.19} \bar{n}_{e,19}^{0.41} \tag{6}$$

where H_H is the so-called confinement factor, I_p is the total plasma current which must be given in MA, P_{tot} must be given in MW, B_T is the toroidal magnetic field, κ is the plasma elongation, $\epsilon = a/R_0$ is the inverse aspect ratio, where a is the tokamak minor radius, M is the effective mass of the plasma in a.m.u., and $\bar{n}_{e,19}$ is the line-average electron density in 10^{19} m^{-3}. The confinement factor H_H is modeled as an uncertain parameter given by

$$H_H = H_H^{\text{nom}} + \delta_{H_H} \tag{7}$$

where H_H^{nom} is a constant, the nominal value of H_H which is known, and δ_{H_H} is an uncertain term. In addition, an uncertain source/sink of power, δ_P, is added to the right-hand side of (4) to account for neglected dynamics such as inefficient heat deposition, unexpected radiative losses, or others. Equation (4) can be rewritten as

$$\frac{dW}{dt} = -\frac{W}{H_H^{\text{nom}} k P_{\text{tot}}^{-0.69}} + P_{\text{tot}} + \delta_W \tag{8}$$

where $\delta_W = W/(k P_{\text{tot}}^{-0.69})[(1/H_H^{nom}) - (1/H_H^{\text{nom}} + \delta_{H_H})] + \delta_P$ is a term that bundles all the uncertain terms of the W subsystem.

Authorized licensed use limited to: LEHIGH UNIVERSITY. Downloaded on July 13,2020 at 21:30:41 UTC from IEEE Xplore. Restrictions apply.

B. Global Toroidal Rotation

The bulk toroidal rotation, Ω_ϕ, is the figure of merit used in this model to characterize the toroidal plasma rotation. It is defined as the average toroidal rotation of the ions inside the plasma, and it is given by

$$\Omega_\phi(t) \triangleq \frac{1}{N_p(t)} \int_{V_p} \langle n_e(\hat{\rho}, t) \rangle \, \omega_\phi(\hat{\rho}, t) dV \tag{9}$$

where N_p is the total number of ions within the plasma, which is approximately calculated as

$$N_p = \bar{n}_e V(\rho_b) \tag{10}$$

where $\bar{n}_e$ is the line-average electron density, and $V(\rho_b)$ is the total plasma volume.

The model proposed in this article for the dynamics of Ω_ϕ is simplified but based on first principles. In the same way that a particle of mass m and position vector $\vec{r}$ would have an angular momentum given by $\vec{L} = \vec{r} \times m(d\vec{r}/dt)$, the plasma is assumed to have an angular momentum Γ in the z-direction given by $\Gamma = m_p R_0^2 \Omega_\phi$, where m_p is the plasma mass contained within the last closed magnetic-flux surface, which neglecting the electrons contribution can be estimated as $m_p = m_D N_p / N_{Av} = m_D \bar{n}_e V(\rho_b)/N_{Av}$, where m_D is the molar mass of the plasma and N_{Av} is Avogadro's number. In this control-oriented model, the plasma is regarded as a particle with the same mass as the total plasma mass, which is rotating around the z-axis with angular velocity $\vec{\Omega}_\phi = \Omega_\phi \vec{z}$, and at a distance R_0. The angular momentum varies in time due to the external torque sources as

$$\frac{d\Gamma}{dt} = R_0^2 \frac{d\left(m_p \Omega_\phi\right)}{dt} = \sum_{i=1}^{N_{\text{NBI}}} T_{\text{NBI},i} + T_{\text{int}} \tag{11}$$

where $T_{\text{NBI},i}$ is the torque injected by the i-th NBI, and T_{int} is a plasma intrinsic-torque source. The model could be easily extended to include other torque sources, such as nonresonant magnetic fields. Expanding the time derivative in (11) and rearranging terms, it is possible to write

$$\frac{d\Omega_\phi}{dt} = -\Omega_\phi \frac{1}{m_p} \frac{dm_p}{dt} + \sum_{i=1}^{N_{\text{NBI}}} \frac{T_{\text{NBI},i}}{m_p R_0^2} + \frac{T_{\text{int}}}{m_p R_0^2}. \tag{12}$$

The first term, $-\Omega_\phi (1/m_p)(dm_p/dt)$, models the decrease of toroidal rotation by diffusion. By defining a global rotation confinement time, τ_{Ω_ϕ}, as $\tau_{\Omega_\phi} \triangleq m_p/(dm_p/dt)$, the Ω_ϕ dynamics (12) can be rewritten as

$$\frac{d\Omega_\phi}{dt} = -\frac{\Omega_\phi}{\tau_{\Omega_\phi}} + \sum_{i=1}^{N_{\text{NBI}}} \frac{T_{\text{NBI},i}}{m_p R_0^2} + \frac{T_{\text{int}}}{m_p R_0^2}. \tag{13}$$

Control-oriented models for τ_{Ω_ϕ}, $T_{\text{NBI},i}$, and T_{int} are employed. First, τ_{Ω_ϕ} is taken as $\tau_{\Omega_\phi} = k_\Omega \tau_E$, where $k_\Omega > 0$ is a dimensionless parameter, which is modeled as a constant. Second, $T_{\text{NBI},i}$ is taken as

$$T_{\text{NBI},i} = k_{\text{NBI},i} P_{\text{NBI},i} \tag{14}$$

where $k_{\text{NBI},i}$ are modeled as constant parameters. Finally, the intrinsic rotation is modeled as a torque source [8], $T_{\text{int}} = k_{\text{int}} W/I_p$, where k_{int} is taken as a constant parameter in this modeling work.

In addition to the uncertainty found in τ_Ω because of H_H, an unknown source/sink of torque δ_T is added on the right-hand side of (13) to account for neglected dynamics, such as inefficient torque injection, uncertainty in the model parameters ($k_{\text{NBI},i}$, k_{int}, and so on), inaccurate measurements of the state/inputs, or others. Equation (13) can be rewritten as

$$\frac{d\Omega_\phi}{dt} = -\frac{\Omega_\phi}{k_\Omega H_H^{\text{nom}} k P_{\text{tot}}{}^{-0.69}} + \sum_{i=1}^{N_{\text{NBI}}} \frac{k_{\text{NBI},i} P_{\text{NBI},i}}{m_p R_0^2} + k_{\text{int}} \frac{W}{I_p m_p R_0^2} + \delta_{\Omega_\phi} \tag{15}$$

where $\delta_{\Omega_\phi} = \Omega_\phi/(k_\Omega k P_{\text{tot}}{}^{-0.69})[1/H_H^{\text{nom}} - (1/H_H^{\text{nom}}) + \delta_{H_H}] + \delta_T$ is a term that bundles all the uncertain terms of the Ω_ϕ subsystem.

C. Summary: State-Space Model

The state-space model for the $\Omega_\phi + W$ system is given by

$$\begin{bmatrix} \dot{\Omega}_\phi \\ \dot{W} \end{bmatrix} = \begin{bmatrix} -\dfrac{\Omega_\phi}{\tau_{\Omega_\phi}^{\text{nom}}} + \sum_i \dfrac{k_{\text{NBI},i} P_{\text{NBI},i}}{m_p R_0^2} + k_{\text{int}} \dfrac{W}{I_p m_p R_0^2} + \delta_{\Omega_\phi} \\ -\dfrac{W}{\tau_E^{\text{nom}}} + \sum_i P_{\text{NBI},i} + P_{EC} + \delta_W \end{bmatrix}$$

or simply as

$$\dot{x} = \begin{bmatrix} f_{\Omega_\phi}(x, u, t, \delta) \\ f_W(x, u, t, \delta) \end{bmatrix} \tag{16}$$

where $x \triangleq [\Omega_\phi, W]^T$ is the state vector, $u \triangleq [P_{\text{NBI},1}, \ldots, P_{\text{NBI},N_{\text{NBI}}}]^T$ is the input vector, $\delta \triangleq [\delta_{H_H}, \delta_P, \delta_T]^T$ is the uncertainties vector, and τ_E^{nom} and $\tau_{\Omega_\phi}^{\text{nom}}$ are the values of τ_E and τ_{Ω_ϕ} with $H_H = H_H^{\text{nom}}$. The explicit dependence with t in the state equation (16) is due to the time-dependent inputs to the model that are assumed to be noncontrollable in this article, i.e., P_{EC}, I_p, and $\bar{n}_e$.

III. Control Design

A. Nominal Control Law via Lyapunov Theory

A nominal control law (i.e., with $\delta = 0$) denoted by u^{nom} is designed with the purpose of simultaneously regulating Ω_ϕ and W. The control objective is to drive x to a target value, $\bar{x} = [\bar{\Omega}_\phi, \bar{W}]^T$, where $\bar{\Omega}_\phi$ and $\bar{W}$ are the rotation and energy targets, respectively. A control law $u^{\text{nom}} = [P_{\text{NBI},1}^{\text{nom}}, \ldots, P_{\text{NBI},N_{\text{NBI}}}^{\text{nom}}]^T$ that stabilizes the nominal system can be obtained by solving the following system of two nonlinear equations:

$$\begin{aligned} f_{\Omega_\phi}(x, u^{\text{nom}}, t, 0) &= -\frac{\bar{\Omega}_\phi + \tilde{\Omega}_\phi}{k_\Omega H_H^{\text{nom}} k \left(\sum_i P_{\text{NBI},i}^{\text{nom}} + P_{EC}\right)^{-0.69}} \\ &\quad + \sum_i \frac{k_{\text{NBI}} P_{\text{NBI},i}^{\text{nom}}}{m_p R_0^2} + k_{\text{int}} \frac{\bar{W} + \tilde{W}}{I_p m_p R_0^2} \\ &= -k_{P,\Omega} \tilde{\Omega}_\phi + \frac{d\bar{\Omega}_\phi}{dt} \end{aligned} \tag{17}$$

Authorized licensed use limited to: LEHIGH UNIVERSITY. Downloaded on July 13,2020 at 21:30:41 UTC from IEEE Xplore. Restrictions apply.

$$f_W(x,u^{\text{nom}},t,0) = -\frac{\bar{W}+\tilde{W}}{H_H^{\text{nom}} k\left(\sum_i P_{\text{NBI},i}^{\text{nom}} + P_{EC}\right)^{-0.69}} + \sum_i P_{\text{NBI},i}^{\text{nom}} + P_{EC} = -k_{P,W}\tilde{W} + \frac{d\bar{W}}{dt} \tag{18}$$

where $k_{P,\Omega} > 0$ and $k_{P,W} > 0$ are constants determined during the controller design, $\tilde{\Omega}_\phi = \Omega_\phi - \bar{\Omega}_\phi$ is the error variable associated with Ω_ϕ, and $\tilde{W} = W - \bar{W}$ is the error variable associated with W. The solution of (17) and (18) provides two constraints for N_{NBI} unknowns.

Under the control law defined by the solution of (17) and (18), the nominal dynamics is reduced to

$$\frac{d\tilde{x}}{dt} = -\begin{bmatrix} k_{P,\Omega} & 0 \\ 0 & k_{P,W} \end{bmatrix}\tilde{x} \tag{19}$$

where $\tilde{x} = [\tilde{\Omega}_\phi, \tilde{W}]^T$. Using the Lyapunov function $V = 1/2\tilde{x}^T\tilde{x} = 1/2\left(\tilde{\Omega}_\phi^2 + \tilde{W}^2\right)$ for the reduced nominal system (19), it is found that

$$\dot{V} = -\tilde{x}^T\begin{bmatrix} k_{P,\Omega} & 0 \\ 0 & k_{P,W} \end{bmatrix}\tilde{x} = -k_{P,\Omega}\tilde{\Omega}_\phi^2 - k_{P,W}\tilde{W}^2. \tag{20}$$

Therefore, the evolution of the nominal system is exponentially stable [9].

B. Robust Control Law via Lyapunov Redesign

In order to ensure robust stability for (16) under the presence of uncertainties ($\delta \neq 0$), an extra term u_{rob} is added to u^{nom} so that $u = u^{\text{nom}} + u^{\text{rob}}$ (i.e., $P_{\text{NBI},i} = P_{\text{NBI},i}^{\text{nom}} + P_{\text{NBI},i}^{\text{rob}}$), where u^{rob} is obtained by means of Lyapunov redesign techniques [9]. First, it is convenient to rewrite (16) as

$$\begin{bmatrix} \dot{\tilde{\Omega}}_\phi \\ \dot{\tilde{W}} \end{bmatrix} = \begin{bmatrix} -\dfrac{d\bar{\Omega}_\phi}{dt} + \dfrac{k_{\text{int}}W}{I_p m_p R_0^2} \\ -\dfrac{d\bar{W}}{dt} + P_{EC} \end{bmatrix} + \begin{bmatrix} -\dfrac{\Omega_\phi}{\tau_{\Omega_\phi}^{\text{nom}}} + \sum_i \dfrac{k_{\text{NBI},i} P_{\text{NBI},i}}{m_p R_0^2} \\ -\dfrac{W}{\tau_E^{\text{nom}}} + \sum_i P_{\text{NBI},i} \end{bmatrix} + \begin{bmatrix} \delta_{\Omega_\phi} \\ \delta_W \end{bmatrix} = F(\tilde{x},t) + \hat{u} + \hat{\delta}(\tilde{x},u,t) \tag{21}$$

where the matrix $F \in \mathbb{R}^{2\times 1}$ lumps the terms that do not depend on u or δ, $\hat{u} \triangleq [-\Omega_\phi/\tau_{\Omega_\phi}^{\text{nom}} + \sum_i k_{\text{NBI},i} P_{\text{NBI},i}/(m_p R_0^2),\ -W/\tau_E^{\text{nom}} + \sum_i P_{\text{NBI},i}]^T$, and $\hat{\delta} \triangleq [\delta_{\Omega_\phi}, \delta_W]^T$ lumps the uncertain terms. Taking (21) and the same Lyapunov function V as before, it is found that

$$\dot{V} = \tilde{x}^T F + \tilde{x}^T\hat{u}^{\text{nom}} + \tilde{x}^T\hat{u}^{\text{rob}} + \tilde{x}^T\hat{\delta} = -\tilde{x}^T\begin{bmatrix} k_{P,\Omega} & 0 \\ 0 & k_{P,W} \end{bmatrix}\tilde{x} + \tilde{x}^T\hat{u}^{\text{rob}} + \tilde{x}^T\hat{\delta} \tag{22}$$

where $\tilde{x}^T(F + \hat{u}^{\text{nom}}) = -\tilde{x}^T\begin{bmatrix} k_{P,\Omega} & 0 \\ 0 & k_{P,W} \end{bmatrix}\tilde{x}$ has been employed, $\hat{u}^{\text{nom}}$ is the value of $\hat{u}$ with $P_{\text{NBI},i} = P_{\text{NBI},i}^{\text{nom}}$, and $\hat{u}^{\text{rob}}$ is the value of $\hat{u}$ with $P_{\text{NBI},i} = P_{\text{NBI},i}^{\text{rob}}$. Taking $\hat{u}^{\text{rob}} = -\eta(\tilde{x})\tilde{x}/\|\tilde{x}\|_2$, for some scalar function $\eta(\tilde{x}) > 0$, (22) becomes

$$\dot{V} = -\tilde{x}^T\begin{bmatrix} k_{P,\Omega} & 0 \\ 0 & k_{P,W} \end{bmatrix}\tilde{x} - \eta(x)\|\tilde{x}\|_2 + \tilde{x}^T\hat{\delta}, \leq -\tilde{x}^T\begin{bmatrix} k_{P,\Omega} & 0 \\ 0 & k_{P,W} \end{bmatrix}\tilde{x} - \eta(x)\|\tilde{x}\|_2 + \|\tilde{x}\|_2\|\hat{\delta}\|_2 \tag{23}$$

and setting $\eta(x) \geq \|\hat{\delta}\|_2 > 0$, it is found that

$$\dot{V} \leq -\tilde{x}^T\begin{bmatrix} k_{P,\Omega} & 0 \\ 0 & k_{P,W} \end{bmatrix}\tilde{x} \tag{24}$$

which ensures that the uncertain system remains exponentially stable [9]. Although $\hat{\delta}$ is not exactly known, it is assumed that an absolute bound to $\|\hat{\delta}\|_2$, denoted by $\hat{\delta}_{\max}$, can be estimated. Therefore, taking $\eta = \hat{\delta}_{\max}$, a robust control law given by $u^{\text{rob}} = -\hat{\delta}_{\max}\tilde{x}/\|\tilde{x}\|_2$ would ensure the exponential stability of the system for all values of $\hat{\delta}$. To make the control law continuous at $\tilde{x} = 0$, using a similar process as showed in [9], the control law is modified as

$$\hat{u}^{\text{rob}} = -\hat{\delta}_{\max}\frac{\tilde{x}}{\|\tilde{x}\|_2}, \quad \text{if } \hat{\delta}_{\max}\|\tilde{x}\|_2 \geq \epsilon_R \tag{25}$$

$$\hat{u}^{\text{rob}} = -\hat{\delta}_{\max}^2\frac{\tilde{x}}{\epsilon_R}, \quad \text{if } \hat{\delta}_{\max}\|\tilde{x}\|_2 < \epsilon_R \tag{26}$$

where $\epsilon_R > 0$ is a design parameter. The control law (25) and (26) does not ensure that the system remains exponentially stable, but it does ensure that $\|\tilde{x}\|_2$ is bounded by a class $\mathcal{K}$ function[1] of ϵ_R as $t \to \infty$. Therefore, it is convenient that ϵ_R is chosen small.

C. Actuator Management via Optimization

It can be noted that (17) and (18) together with (25) and (26) is a nonlinear system of four equations with 2 N_{NBI} unknowns, $P_{\text{NBI},i}^{\text{nom}}$, and $P_{\text{NBI},i}^{\text{rob}}$, for $i = 1,\ldots,N_{\text{NBI}}$, which are the components of u^{nom} and u^{rob}. The solution of the system[2] depends on N_{NBI}. If $N_{\text{NBI}} = 1$, the system is overconstrained, indicating that, in general, it is not possible to control both Ω_ϕ and W simultaneously. If $N_{\text{NBI}} = 2$, there are the same number of unknowns as equations, and it is possible to regulate both Ω_ϕ and W at the same time as long as the NBI configuration allows to do so. Finally, if $N_{\text{NBI}} > 2$, the system is underconstrained, and extra conditions may need to be imposed in order to univocally determine $P_{\text{NBI},i}$.

A way of imposing extra conditions is to write the problem as an optimization problem. It is chosen that, at every time step, an objective function of the norm of $\tilde{u} \triangleq u - u_{\text{FF}}$ is minimized (u_{FF} is a reference or feedforward input), i.e., the difference between u and u_{FF} is taken as small as possible. In addition, the constraints from the control laws (17)–(18), (25)–(26), and the physical saturation levels are imposed. The components of $\tilde{u}$ (i.e., $\tilde{P}_{\text{NBI},i}$) are free variables of the optimization problem, which is given by

[1] A function $f(x)$ belongs to class $\mathcal{K}$ iff: 1) $f(0) = 0$ and 2) it is an strictly increasing function of x.

[2] The discussion and/or formal demonstration of the existence and/or unicity of solutions for this nonlinear system is left aside in this work. It is assumed that the system has a unique solution if $N_{\text{NBI}} > 1$.

Authorized licensed use limited to: LEHIGH UNIVERSITY. Downloaded on July 13,2020 at 21:30:41 UTC from IEEE Xplore. Restrictions apply.

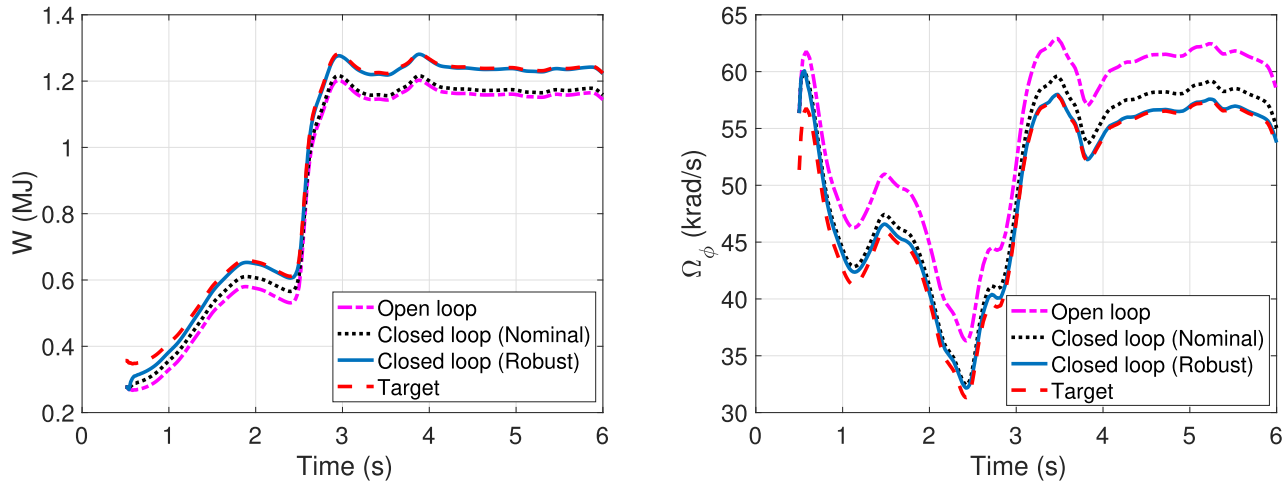

Fig. 2. State evolution in open loop (magenta dashed-dotted line) and closed loop under the nominal (black dotted line) and robust (blue solid line) control laws in 1-D simulations, together with the corresponding targets (red dashed line).

$$\min_{\tilde{u}} J(\tilde{u}) = \min_{\tilde{u}} \tilde{u}^T Q \tilde{u} \tag{27}$$

$$f_{\Omega_\phi}(x, u^{\text{nom}}, t, 0) = -k_{P,\Omega}\tilde{\Omega}_\phi + \frac{d\bar{\Omega}_\phi}{dt} \tag{28}$$

$$f_W(x, u^{\text{nom}}, t, 0) = -k_{P,W}\tilde{W} + \frac{d\bar{W}}{dt}, \tag{29}$$

$$-\frac{\Omega_\phi}{\tau^{\text{nom}}_{\Omega_\phi}\left(P^{\text{rob}}_{\text{NBI},i}\right)} + \sum_i \frac{k_{\text{NBI},i} P^{\text{rob}}_{\text{NBI},i}}{m_p R_0^2} = -\hat{\delta}_{\max}\frac{\tilde{\Omega}_\phi}{\epsilon} \tag{30}$$

$$-\frac{W}{\tau^{\text{nom}}_E\left(P^{\text{rob}}_{\text{NBI},i}\right)} + \sum_i P^{\text{rob}}_{\text{NBI},i} = -\hat{\delta}_{\max}\frac{\tilde{W}}{\epsilon} \tag{31}$$

$$\tilde{u} \in \tilde{\mathcal{U}}, \tag{32}$$

where $Q \in \mathbb{R}^{N_{\text{NBI}} \times N_{\text{NBI}}} \geq 0$ is a design matrix, $\epsilon = \|[\tilde{\Omega}_\phi, \tilde{W}]^T\|_2$ if $\hat{\delta}_{\max}\|[\tilde{\Omega}_\phi, \tilde{W}]^T\|_2 \geq \epsilon_R$, $\epsilon = \epsilon_R/\hat{\delta}_{\max}$ if $\hat{\delta}_{\max}\|[\tilde{\Omega}_\phi, \tilde{W}]^T\|_2 < \epsilon_R$, and $\tilde{\mathcal{U}}$ is the set of feasible NBI power deviations. The optimization problem (27)–(32) serves as an actuator manager that determines the inputs that fulfill the control law and saturation constraints and minimize $J(\tilde{u})$.

IV. Simulation Study

In this section, the control scheme previously introduced is tested in simulations for a DIII-D scenario. The scenario corresponds to shot 147 634, in which eight NBIs are available. These are grouped in three sets of NBIs (i.e., $N_{\text{NBI}} = 3$) as follows.

1) *Group 1:* It consists of four co-current on-axis NBIs. This group's total power, $P_{\text{NBI},1}$, is denoted by $P_{\text{CO-ON}}$.
2) *Group 2:* It consists of two co-current off-axis NBIs. This group's total power, $P_{\text{NBI},2}$, is denoted by $P_{\text{CO-OFF}}$.
3) *Group 3:* It consists of two counter-current NBIs. This group's total power, $P_{\text{NBI},3}$, is denoted by P_{COUNTER}.

Grouping the NBIs is convenient to reduce the size of (27)–(32) and is necessary to not overestimate the actuation capability in DIII-D. Relevant machine parameters and model constants are $R_0 = 1.80$ m, $B_T = 1.65$ T, $a = 0.60$ m, $\kappa = 1.7$, $M = 2$ a.m.u., $H_H^{\text{nom}} = 1.4$, $k_\Omega = 1$, $k_{\text{int}} = 3$ N·m MA/MJ, $k_{\text{NBI},i} = 1$ N·m/MW for each cocurrent on-axis NBI, $k_{\text{NBI},i} = 0.7$ N·m/MW for each cocurrent off-axis NBI, and $k_{\text{NBI},i} = -1$ N·m/MW for each counter-current NBI. The saturation limits are $P_{\text{NBI},i} \in [0, 2.5]$ MW.

For simulation testing, the Control-Oriented Transport Simulator (COTSIM) code is employed. COTSIM is a 1-D code for control testing and simulation that evolves T_e and ω_ϕ using the electron heat-transport equation (EHTE) and the toroidal rotation equation (TRE), which are given by

$$\frac{\partial\left(\frac{3}{2}n_e T_e\right)}{\partial t} = \frac{1}{\rho_b^2 \hat{\rho}\hat{H}}\frac{\partial}{\partial\hat{\rho}}\left(\frac{\hat{G}\hat{H}^2}{\hat{F}}\chi_e n_e \frac{\partial T_e}{\partial\hat{\rho}}\right) + Q_e \tag{33}$$

$$m_i\langle r^2\rangle\frac{\partial(n_i\omega_\phi)}{\partial t} = \frac{1}{\hat{\rho}\hat{H}}\frac{\partial}{\partial\hat{\rho}}\left(f_\phi\chi_\phi n_i\frac{\partial\omega_\phi}{\partial\hat{\rho}}\right) + t_\omega \tag{34}$$

where χ_e and χ_ϕ are the electron heat and toroidal momentum diffusivities, respectively, m_i is the ion mass, Q_e and t_ω are the electron-heat and ion-torque deposition, respectively, and $\hat{F}$, $\hat{G}$, $\hat{H}$, $\langle r^2\rangle$, and f_ϕ are fixed profiles corresponding to a particular magnetic configuration. Approximate models for n_e and n_i are employed, $n_e = n_e^{\text{prof}}\bar{n}_e$ and $n_i = n_i^{\text{prof}}\bar{n}_i$, where n_e^{prof} and n_i^{prof} are fixed profiles that characterize the spatial distribution of the electron and ion densities, respectively, and $\bar{n}_e$ and $\bar{n}_i$ are the line-average electron and ion densities, respectively. For Q_e and t_ω, COTSIM employs the following control-oriented models for this simulation study, $Q_e = \sum_i Q^{\text{prof}}_{\text{NBI},i}P_{\text{NBI},i} + Q^{\text{prof}}_{EC}P_{EC}$, and $t_\omega = \sum_i t^{\text{prof}}_{\text{NBI},i}P_{\text{NBI},i} + t_{\text{int}}$, where $Q^{\text{prof}}_{\text{NBI},i}$ and Q^{prof}_{EC} are fixed profiles that characterize the electron-heating spatial deposition for the i-th NBI and EC, respectively, $t^{\text{prof}}_{\text{NBI},i}$ is a profile that depends on both T_e and n_i and characterizes the torque spatial deposition, and t_{int} is the intrinsic torque, which is a function of E and, therefore, of T_e as well. Also, Bohm-like models [10] are utilized for χ_e and χ_ϕ, as given by $\chi_{(\cdot)} = T_e/B_T(a\nabla p_e/p_e)^{\lambda_1}q^{\lambda_2}$, where $p_e \triangleq n_e K T_e$ is the electron pressure, q is the safety factor, a measure of the helicity of the magnetic field lines in a tokamak [1] whose evolution is estimated in COTSIM by means of the magnetic diffusion equation [11], and λ_1 and λ_2 are constant parameters. Therefore, it can be appreciated that the EHTE and TRE models are coupled by means of χ_e, χ_ϕ, Q_e, and t_ω, representing a substantial increase in complexity with respect to the models employed for control synthesis.

Authorized licensed use limited to: LEHIGH UNIVERSITY. Downloaded on July 13,2020 at 21:30:41 UTC from IEEE Xplore. Restrictions apply.

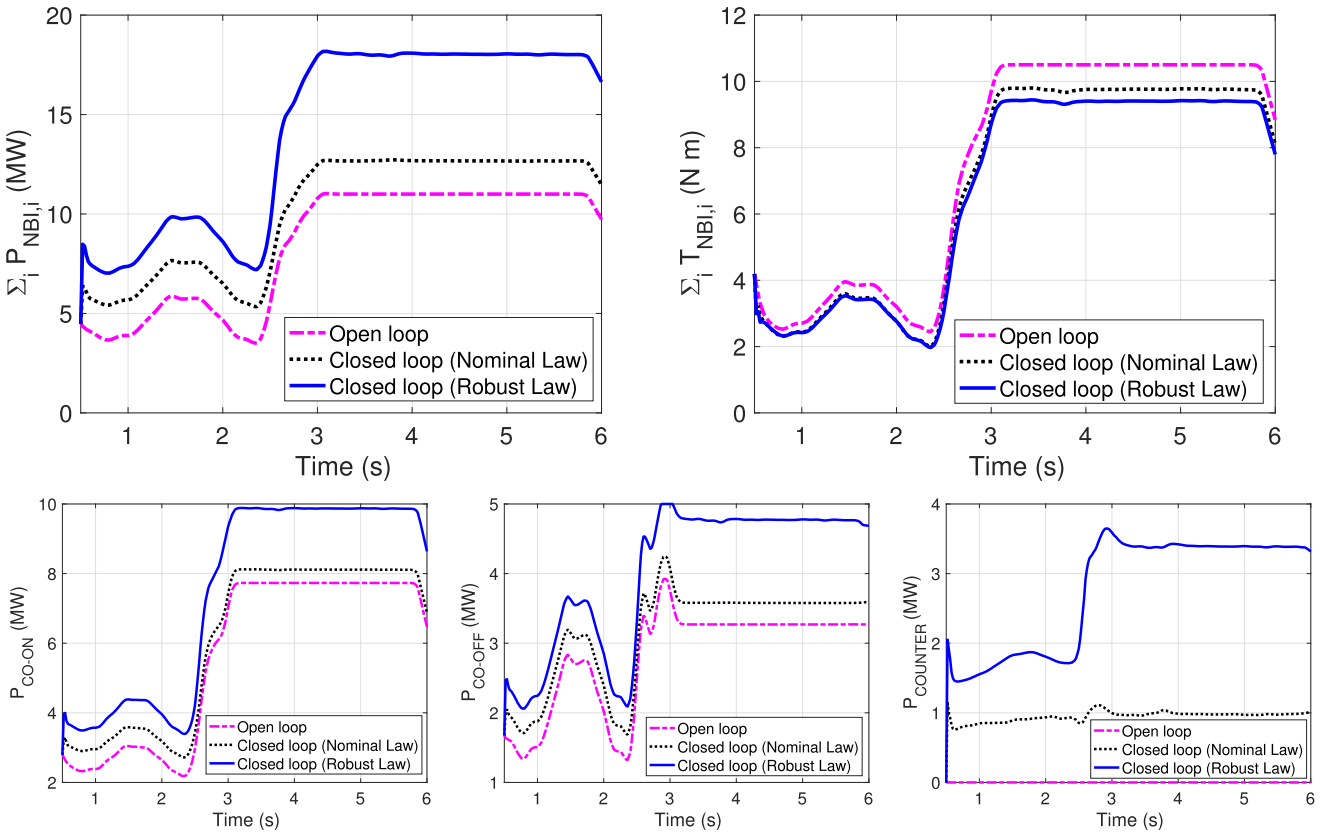

Fig. 3. NBI power (P_{NBI}) and torque (T_{NBI}) evolutions in open loop (magenta dashed-dotted line) and closed loop under the nominal (black dotted line) and robust (blue solid line) control laws, together with ON-axis cocurrent NBIs ($P_{\mathrm{CO\text{-}ON}}$), OFF-axis cocurrent NBIs ($P_{\mathrm{CO\text{-}OFF}}$), and counter-current NBI's (P_{COUNTER}) in 1-D simulations.

Several simulations are run for this article. First, an open-loop simulation is carried out with the experimental inputs, u_{exp}, corresponding to shot 147 634. The state evolution obtained in this open-loop simulation is denoted by x_{exp}. A target $\bar{x} = [\bar{\Omega}_\phi, \bar{W}]^T$ is created based on the open-loop simulation. The Ω_ϕ target is given by $\bar{\Omega}_\phi = (\Omega_\phi)_{\mathrm{exp}} - 5$ krad/s, whereas the W target is given by $\bar{W} = W_{\mathrm{exp}} + 0.08$ MJ. Second, a closed-loop simulation is run under the nominal control law ($u = u^{\mathrm{nom}}$). Finally, a closed-loop simulation is run under the robust control law ($u = u^{\mathrm{nom}} + u^{\mathrm{rob}}$). To solve (27)–(32), $u_{FF} = u_{\mathrm{exp}}$ is taken.

Fig. 2 shows the state evolution, x, in open loop (i.e., x_{exp}) and closed loop under the nominal and robust control laws, together with the target $\bar{x}$. Fig. 3 shows the time evolution of the total NBI power, $\sum_i P_{\mathrm{NBI},i}$, and total NBI torque, $\sum_i T_{\mathrm{NBI},i}$ (as computed by the 0-D model (14)), in open-loop (i.e., calculated from u_{exp}) and closed-loop simulations. Fig. 3 also shows the time evolution of $P_{\mathrm{NBI},i}$ grouped, as indicated earlier (co-current on-axis NBI, $P_{\mathrm{CO\text{-}ON}}$, co-current off-axis NBI, $P_{\mathrm{CO\text{-}OFF}}$, and counter-current NBI, P_{COUNTER}). Fig. 2 shows that the nominal law drives x closer to $\bar{x}$ compared with the open-loop evolution, but x does not converge to the target $\bar{x}$ within the simulation time. It can be seen that the robust controller drives x much closer to the target $\bar{x}$ (with a small error associated with ϵ_R) than the nominal controller. Fig. 3 shows how $\sum_i P_{\mathrm{NBI},i}$ is increased by both the nominal and robust controllers to achieve the target $\bar{W} > W_{\mathrm{exp}}$. The robust controller requests a higher $\sum_i P_{\mathrm{NBI},i}$ than the nominal controller (about 5 MW more), which seems to be the reason for its better performance. Also, as $\bar{\Omega}_\phi < \Omega_{\mathrm{exp}}$, the NBI torque is decreased by both control laws. As before, the robust controller is more aggressive and requests a lower NBI torque than the nominal controller. Fig. 3 shows that, when using the robust law, all $P_{\mathrm{NBI},i}$ are very close to saturation, and $P_{\mathrm{CO\text{-}OFF}}$ even saturates for a small period of time. This happens as a result of a very demanding target $\bar{x}$.

V. Conclusion

A robust controller for simultaneous energy and toroidal rotation control in tokamaks has been presented. It is a model-based, 0-D controller synthesized from nonlinear, control-oriented models. The controller is composed of a nominal control law and a robust control law, both designed using Lyapunov techniques. Both the nominal and the robust controllers have been tested in 1-D simulations using the COTSIM code for a particular DIII-D scenario. However, the controller design procedure is independent of the tokamak and/or scenario in question. If the robust control law is activated, the controller shows a better performance compared with the nominal control law working on its own. Future work may include the integration of new scalar variables in the control scheme and experimental testing in the DIII-D tokamak.

Authorized licensed use limited to: LEHIGH UNIVERSITY. Downloaded on July 13,2020 at 21:30:41 UTC from IEEE Xplore. Restrictions apply.

DISCLAIMER

This report was prepared as an account of work sponsored by an agency of the United States Government. Neither the United States Government nor any agency thereof, nor any of their employees, makes any warranty, express or implied, or assumes any legal liability or responsibility for the accuracy, completeness, or usefulness of any information, apparatus, product, or process disclosed, or represents that its use would not infringe privately owned rights. Reference herein to any specific commercial product, process, or service by trade name, trademark, manufacturer, or otherwise does not necessarily constitute or imply its endorsement, recommendation, or favoring by the United States Government or any agency thereof. The views and opinions of authors expressed herein do not necessarily state or reflect those of the United States Government or any agency thereof.

REFERENCES

[1] J. Wesson, *Tokamaks*. Oxford, U.K.: Clarendon, 1984.
[2] J. T. Scoville, D. A. Humphreys, J. R. Ferron, and P. Gohil, "Simultaneous feedback control of plasma rotation and stored energy on the DIII-D tokamak," *Fusion Eng. Des.*, vol. 82, nos. 5–14, pp. 1045–1050, Oct. 2007.
[3] W. Wehner, J. Barton, and E. Schuster, "Combined rotation profile and plasma stored energy control for the DIII-D tokamak via MPC," in *Proc. Amer. Control Conf. (ACC)*, May 2017, pp. 4872–4877.
[4] M. D. Boyer *et al.*, "Feedback control of stored energy and rotation with variable beam energy and perveance on DIII-D," *Nucl. Fusion*, vol. 59, no. 7, Jul. 2019, Art. no. 076004.
[5] I. R. Goumiri *et al.*, "Simultaneous feedback control of plasma rotation and stored energy on NSTX-U using neoclassical toroidal viscosity and neutral beam injection," *Phys. Plasmas*, vol. 24, no. 5, May 2017, Art. no. 056101.
[6] A. Pajares and E. Schuster, "Actuator management via real-time optimization for integrated control in tokamaks," in *Proc. 46th EPS Conf. Plasma Phys.*, 2019, p. 1.
[7] N. A. Uckan, "Confinement capability of ITER-EDA design," in *Proc. 15th IEEE/NPSS Symp. Fusion Eng.*, vol. 1, 1993, pp. 183–186.
[8] W. M. Solomon *et al.*, "Mechanisms for generating toroidal rotation in tokamaks without external momentum input," *Phys. Plasmas*, vol. 17, no. 5, May 2010, Art. no. 056108.
[9] H. Khalil, *Nonlinear Systems*, 3rd ed. Upper Saddle River, NJ, USA: Prentice-Hall, 2001.
[10] M. Erba, T. Aniel, V. Basiuk, A. Becoulet, and X. Litaudon, "Validation of a new mixed Bohm/gyro-Bohm model for electron and ion heat transport against the ITER, tore supra and START database discharges," *Nucl. Fusion*, vol. 38, no. 7, pp. 1013–1028, Jul. 1998.
[11] F. L. Hinton and R. D. Hazeltine, "Theory of plasma transport in toroidal confinement systems," *Rev. Modern Phys.*, vol. 48, no. 2, pp. 239–308, Apr. 1976.

Andres Pajares received the bachelor's and M.Sc. degrees in aerospace engineering from the University of Seville, Seville, Spain, in 2012, and the Ph.D. degree in mechanical engineering from Lehigh University, Bethlehem, PA, USA, in 2019.

He is currently a Post-Doctoral Researcher within the Lehigh University Plasma Control Laboratory. His work focuses on the development and experimental testing of plasma-control algorithms at the DIII-D National Fusion Facility in San Diego, where he is permanently stationed. His research interests include physics-based plasma modeling and the design of integrated algorithms for plasma-control applications.

Eugenio Schuster received the Ph.D. degree from the University of California at San Diego, San Diego, CA, USA, in 2004.

He is currently a Professor with the Department of Mechanical Engineering and Mechanics, Lehigh University, Bethlehem, PA, USA. He is an Expert in nuclear-fusion plasma control and leads the Lehigh University Plasma Control Laboratory.

Prof. Schuster has been appointed as a Scientist Fellow in Plasma Control by the ITER Organization. Moreover, he has been designated by the U.S. Department of Energy (DOE) as an Expert Member of the Integrated Operation Scenarios (IOS) Topical Group within the International Tokamak Physics Activity (ITPA). He has served as Leader of the Operations and Control Topical Group within the U.S. Burning Plasma Organization (BPO) and as the Founder Chair of the Technical Committee on Power Generation within the IEEE Control Systems Society. He was a recipient of the National Science Foundation (NSF) CAREER Award for his work on Nonlinear Control of Plasmas in Nuclear Fusion.

Authorized licensed use limited to: LEHIGH UNIVERSITY. Downloaded on July 13,2020 at 21:30:41 UTC from IEEE Xplore. Restrictions apply.